

A model for the evolution of the thermal bar system

D. E. Farrow

Mathematics & Statistics, Murdoch University, Murdoch, WA 6163, Australia

Abstract

A new framework for modelling the evolution of the thermal bar system in a lake is presented. The model assumes that the thermal bar is located between a deeper region where spring warming leads to overturning of the entire water column and a near shore shallower region where a stable surface layer is established. In this model the thermal bar moves out slightly more quickly than predicted by a simple thermal balance.

Introduction

At the end of winter, the temperature of the water in many temperate lakes is less than $T_m = 4^\circ\text{C}$; the temperature of maximum density. As spring progresses the near shore shallow waters warm more rapidly than the deeper parts. The 4°C isotherm propagates out from the shore and to either side of it different conditions prevail. In the deeper regions the heating destabilises the water column and active mixing occurs. In the shallows the heating leads to a stable stratification. The boundary between these two regions is called the thermal bar.

Previous modelling of the thermal bar system has fallen into two broad categories. The first considers in detail the heat transfer in the lake. By distributing the surface heat flux over the local depth [4] showed that for constant bottom slope the thermal bar moves out from the shore at a constant speed given by

$$\text{Propagation Speed} = \frac{I_0}{\rho_0 C_p A \Delta T_0} \quad (1)$$

where I_0 is the surface heat flux, ρ_0 is the reference density, C_p is the specific heat, A is the bottom slope, $\Delta T_0 = T_m - T_0$ and T_0 is the initial temperature of the lake. This result has been generalised [8] to include horizontal heat transfer in the vicinity of the thermal bar. This additional heat transfer leads to the thermal bar propagating more quickly than (1). The second category has focussed on the general circulation associated with the thermal bar system. These include the quasi-steady state model of [3] and the unsteady asymptotic results of [5, 6]. The models show how inertia and advection can lead to the thermal bar propagating out from the shore either more slowly or more quickly than (1).

A different approach is used here. The framework for the model is that the position of the thermal bar is at the boundary between the stably stratified shallow region and the deeper unstable region. Thus the model focuses on the stability of the local water column rather than considering the lake system as a whole and ignores any horizontal transfer of heat or momentum.

Model formulation

The thermal bar system is modelled by the natural convection of a fluid contained in the semi-infinite two dimensional triangular domain bounded by the lines $\tilde{z} = 0$ and $\tilde{z} = -A\tilde{x}$ in the (\tilde{x}, \tilde{z}) -plane. The domain and coordinate system are shown in fig 1. The flow is driven by a surface heat flux $I_0 \text{Wm}^{-2}$. The precise mechanism whereby the heat enters the system is specified below.

For temperatures near 4°C , the density/temperature relationship

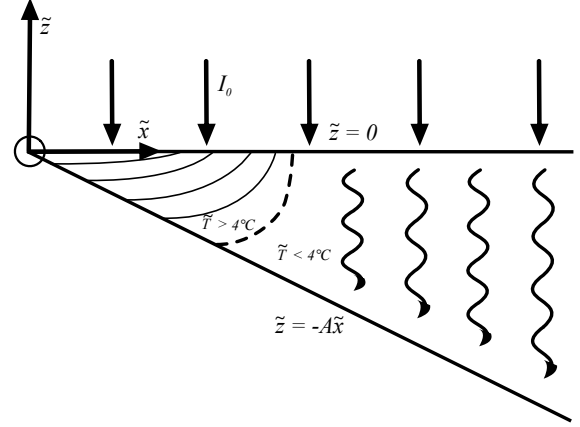


Figure 1: Schematic of flow domain showing conceptual flow structure of thermal bar system.

is well approximated by

$$\rho = \rho_m(1 - \beta(\tilde{T} - T_m)^2) \quad (2)$$

where ρ_m is the maximum density at the maximum density temperature T_m and $\beta \approx 6.8 \times 10^{-6} \text{ }^\circ\text{C}^{-2}$.

For the thermal bar the main heating mechanism is via the absorption of light. As light at a particular wavelength is absorbed with depth its intensity drops according to Beer's law,

$$I(\tilde{z}) = I_0 \exp(-\tilde{\eta}\tilde{z}) \quad (3)$$

where $\tilde{\eta} \text{m}^{-1}$ is the attenuation coefficient. It is assumed here that the light can be characterised by a single attenuation coefficient. The volumetric heating term Q is then

$$Q = \frac{I_0 \tilde{\eta}}{\rho_m C_p} \exp(-\tilde{\eta}\tilde{z}) \quad (4)$$

where C_p is the specific heat of water.

The model is non-dimensionalised following [5]:

$$\tilde{T} - T_0 \sim \Delta T_0 = T_m - T_0 \quad (5)$$

$$\tilde{x} \sim l = \nu \Delta T_0 \rho_0 C_p / (A I_0) \quad (6)$$

$$\tilde{z} \sim h = \nu \Delta T_0 \rho_0 C_p / I_0 \quad (7)$$

$$\tilde{t} \sim \tau = \nu (\Delta T_0 \rho_0 C_p / I_0)^2 \quad (8)$$

$$\tilde{u} \sim U = \frac{A R a h}{\sigma \tau} \quad (9)$$

$$\tilde{w} \sim A U \quad (10)$$

where $\sigma = \nu/\kappa$ is the Prandtl number and Ra is the Rayleigh number given by

$$Ra = \frac{g \Delta \rho_0 h^3}{\rho_m \nu \kappa} \quad (11)$$

The dimensionless equations are then

$$u_t + A^2 Ra(uu_x + wu_z)/\sigma = -p_x + A^2 u_{xx} + u_{zz} \quad (12)$$

$$w_t + A^2 Ra(uw_x + ww_z)/\sigma = -p_z/A^2 + A^2 w_{xx} + w_{zz} + (1-T)^2/A^2 \quad (13)$$

$$T_t + A^2 Ra(uT_x + wT_z)/\sigma = (A^2 T_{xx} + T_{zz})/\sigma + \eta e^{\eta z} \quad (14)$$

$$u_x + w_z = 0 \quad (15)$$

where $\eta = h\tilde{\eta}$ is the dimensionless attenuation coefficient and all variables are now non-dimensional. The boundaries are $z = 0$ and $z = -x$ at which the boundary conditions are

$$u_z = w = T_z = 0 \quad \text{on} \quad z = 0 \quad (16)$$

$$u = w = A^2 T_x + T_z = 0 \quad \text{on} \quad z = -x. \quad (17)$$

The initial conditions are $u = w = T = 0$ at $t = 0$.

The parameter A is small which can be exploited to obtain an asymptotic solution as $A \rightarrow 0$ (see, for example, [5]). Letting $A \rightarrow 0$ yields a system of equations for the $O(A^0)$ solution (denoted by superscripts (0))

$$u_t^{(0)} = -p_x^{(0)} + u_{zz}^{(0)} \quad (18)$$

$$0 = -p_z^{(0)} + (1-T^{(0)})^2 \quad (19)$$

$$T_t^{(0)} = T_{zz}^{(0)}/\sigma + \eta e^{\eta z} \quad (20)$$

$$u_x^{(0)} + w_z^{(0)} = 0 \quad (21)$$

with the boundary conditions

$$u_z^{(0)} = w^{(0)} = T_z^{(0)} = 0 \quad \text{on} \quad z = 0 \quad (22)$$

$$u^{(0)} = w^{(0)} = T_z^{(0)} = 0 \quad \text{on} \quad z = -x \quad (23)$$

and the initial conditions $u^{(0)} = w^{(0)} = T^{(0)} = 0$ at $t = 0$.

$T^{(0)}$ can be determined independently and is the solution of a straightforward one dimensional conduction problem:

$$T^{(0)}(x, z, t) = \frac{t}{x}(1 - e^{-\eta x}) + \sigma \left[z - e^{\eta z}/\eta + \frac{z^2}{2x}(1 - e^{-\eta x}) + \frac{1}{\eta^2 x}(1 - e^{-\eta x}) + \frac{x}{6}(2 + e^{-\eta x}) \right] - \frac{2\eta^2 \sigma}{x} \sum_{n=1}^{\infty} \left(\frac{x}{n\pi} \right)^2 \frac{1 - (-1)^n e^{-\eta x}}{\eta^2 + (n\pi/x)^2} e^{-\left(\frac{n\pi}{x}\right)^2 \frac{t}{\sigma}} \cos\left(\frac{n\pi z}{x}\right). \quad (24)$$

The problem for $u^{(0)}$ is hard to solve as it involves the forcing term $(1 - T^{(0)})^2$ where $T^{(0)}$ is an infinite series. The stability problem discussed below is independent of $u^{(0)}$ so no attempt is made to find $u^{(0)}$.

The stability problem

The $A \rightarrow 0$ solution is perturbed in the following way

$$u = u^{(0)} + \frac{\varepsilon}{A} U(\xi, z, t) \quad (25)$$

$$w = w^{(0)} + \frac{\varepsilon}{A^2} W(\xi, z, t) \quad (26)$$

$$p = p^{(0)} + \varepsilon P(\xi, z, t) \quad (27)$$

$$T = T^{(0)} + \varepsilon \Theta(\xi, z, t) \quad (28)$$

where $\varepsilon \ll 1$ is the perturbation parameter and $\xi = x/A$ is a rescaled horizontal coordinate.

Substitution yields evolution equations for the perturbation quantities,

$$U_t = -P_\xi + U_{\xi\xi} + U_{zz} \quad (29)$$

$$W_t = -P_z + W_{\xi\xi} + W_{zz} - 2\Theta(1 - T^{(0)}) \quad (30)$$

$$\sigma \Theta_t + Ra W T_z^{(0)} = (\Theta_{\xi\xi} + \Theta_{zz}) \quad (31)$$

$$U_\xi + W_z = 0. \quad (32)$$

The boundary conditions become

$$U_z = W = \Theta_z = 0 \quad \text{on} \quad z = 0 \quad (33)$$

$$U = W = \Theta_z = 0 \quad \text{on} \quad z = -x. \quad (34)$$

Introducing a streamfunction with $U = -\Psi_z$ and $W = \Psi_\xi$ and eliminating P from (29)–(32) yields

$$(\partial^2/\partial\xi^2 + \partial^2/\partial z^2)\Psi_t = (\partial^2/\partial\xi^2 + \partial^2/\partial z^2)^2\Psi - 2\Theta_\xi(1 - T^{(0)}) \quad (35)$$

$$\sigma \Theta_t + Ra \Psi_\xi T_z^{(0)} = (\partial^2/\partial\xi^2 + \partial^2/\partial z^2)\Theta. \quad (36)$$

The remainder of the stability analysis makes the ‘‘frozen time’’ assumption with respect to the background temperature structure. It is assumed that the background temperature is steady with respect to the evolution of the perturbation quantities.

The perturbation quantities are assumed to take the form

$$\Psi = \mathcal{R}\{ik\psi(z)e^{st+ik\xi}\} \quad \text{and} \quad \Theta = \mathcal{R}\{\theta(z)e^{st+ik\xi}\} \quad (37)$$

where s is the instantaneous growth rate, k is the wavenumber of the disturbance and i is the imaginary unit. Substitution yields

$$(D^2 - k^2 - s)(D^2 - k^2)\psi = 2\theta(1 - T^{(0)}) \quad (38)$$

$$(D^2 - k^2 - \sigma s)\theta = -Ra_c(x, t)k^2\psi DT^{(0)} \quad (39)$$

where $D \equiv d/dz$. The boundary conditions on ψ and θ are

$$D\theta = \psi = D^2\psi = 0 \quad \text{on} \quad z = 0 \quad (40)$$

$$D\theta = \psi = D\psi = 0 \quad \text{on} \quad z = -x. \quad (41)$$

Specifying particular values for k and s , (38) and (39) along with the associated boundary conditions constitute an eigenvalue problem for $Ra_c(x, t)$ where, as implied by the notation, the value will depend on x and t which serve to specify the local conditions. The focus in this paper is on the boundary between the stable ($s < 0$) and unstable ($s > 0$) regions. Thus the growth rate s is set to zero and the remainder of the stability analysis concentrates on the marginally stable case. The problem is now one of finding the smallest positive eigenvalue Ra_c over all possible wavenumbers. This eigenvalue is the critical Rayleigh number below which localised disturbances are damped.

Solution for $k \rightarrow 0$

Unfortunately, terms appear in (38) and (39) where ψ and θ are multiplied by $T^{(0)}$ and $DT^{(0)}$ which are complicated functions of z . However, [1] have shown that for the case where the background vertical density gradient is constant and with insulated boundary conditions like those that apply here, the critical wave-number k_c at which Ra_c occurs is $k_c = 0$. Even though in the current case where the density gradient is not linear, this

property can be exploited to find an expression for Ra_c analytically, at least for part of the domain.

Following [7], ψ , θ and Ra_c are expanded according to

$$\psi = \psi_0 + k^2\psi_2 + \dots \quad (42)$$

$$\theta = \theta_0 + k^2\theta_2 + \dots \quad (43)$$

$$Ra_c = Ra_{c0} + k^2Ra_{c2} + \dots \quad (44)$$

where the symmetry of the problem has been used to eliminate odd powers of k . Substitution into (38) and (39) and taking the lowest order in k yields

$$D^4\psi_0 = 2\theta_0(1 - T^{(0)}) \quad (45)$$

$$D^2\theta_0 = 0 \quad (46)$$

for which the solution is $\theta_0 = 1$ and

$$\begin{aligned} u_0 = -D\psi_0 = & \left[\frac{t}{x} (1 - e^{-\eta x}) - 1 \right. \\ & + \sigma \left[\frac{1}{\eta^2 x} (1 - e^{-\eta x}) + \frac{x}{6} (2 + e^{-\eta x}) \right] \times \left(\frac{-z^3}{3} - \frac{3z^2 x}{8} + \frac{x^3}{24} \right) \\ & - \sigma \left(\frac{z^4}{12} - \frac{z^2 x^2}{10} + \frac{x^4}{60} \right) - \frac{\sigma}{2x} (1 - e^{-\eta x}) \left(\frac{z^5}{30} + \frac{z^2 x^3}{24} - \frac{x^5}{120} \right) \\ & - 2\sigma \left[\frac{z}{\eta^3} - \frac{1}{\eta^4} e^{\eta z} + \frac{3z^2}{4\eta^5 x^3} \left[2\eta x e^{-\eta x} - 2(1 - e^{-\eta x}) + \eta^2 x^2 \right] \right. \\ & \quad \left. - \frac{1}{4\eta^5 x} \left[2\eta x e^{-\eta x} - 6(1 - e^{-\eta x}) - \eta^2 x^2 \right] \right] \\ & - \frac{4\sigma\eta^2}{x} \sum_{n=1}^{\infty} \left(\frac{x}{n\pi} \right)^2 \frac{1 - (-1)^n e^{-\eta x}}{\eta^2 + (n\pi/x)^2} \exp \left(- \left(\frac{n\pi}{x} \right)^2 \frac{t}{\sigma} \right) \\ & \times \left[\left(\frac{x}{n\pi} \right)^3 \sin \left(\frac{n\pi}{x} z \right) - z \left(\frac{x}{n\pi} \right)^2 \right. \\ & \left. - \frac{1}{4} \left(\frac{x}{n\pi} \right)^4 \left[\left(\frac{3z^2}{x^3} + \frac{1}{x} \right) n^2 \pi^2 + \left(\frac{6z^2}{x^3} - \frac{6}{x} \right) (1 - (-1)^n) \right] \right]. \end{aligned} \quad (47)$$

A solvability condition at the next order in k yields Ra_{c0} ,

$$Ra_{c0} = \left[\frac{1}{2x} \left(u_0 D^2 u_0|_{z=0} + \frac{1}{2} (Du_0)^2|_{z=-x} \right) \right]^{-1}. \quad (48)$$

Numerical Solution

The stability problem (38)–(41) is solved numerically using a shooting method [2]. A vector function $Y = (\psi, D\psi, D^2\psi, D^3\psi, \theta, D\theta)^T$ is introduced so that (38) and (39) can be written as

$$DY = KY \quad (49)$$

where K is a 6×6 matrix

For fixed x and t , (49) is integrated from $z = -x$ to $z = 0$ using the MATLAB routine `ode45` for three different initial conditions $Y(-x) = (0, 0, 1, 0, 0, 0)^T$, $Y(-x) = (0, 0, 0, 1, 0, 0)^T$ and $Y(-x) = (0, 0, 0, 0, 1, 0)^T$. These solutions are labelled Y_1 , Y_2 and Y_3 respectively and they all satisfy the boundary conditions at $z = -x$. The general solution for Y that satisfies all the boundary conditions at $z = 0$ will then be the linear combination $Y = \alpha_1 Y_1 + \alpha_2 Y_2 + \alpha_3 Y_3$. The solution Y must satisfy the boundary conditions at $z = 0$ which can be written

$$\begin{pmatrix} \psi_1(0) & \psi_2(0) & \psi_3(0) \\ D^2\psi_1(0) & D^2\psi_2(0) & D^2\psi_3(0) \\ D\theta_1(0) & D\theta_2(0) & D\theta_3(0) \end{pmatrix} \begin{pmatrix} \alpha_1 \\ \alpha_2 \\ \alpha_3 \end{pmatrix} = \begin{pmatrix} 0 \\ 0 \\ 0 \end{pmatrix}. \quad (50)$$

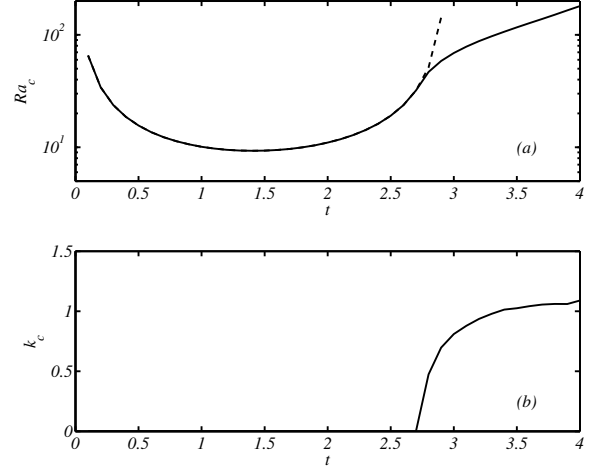


Figure 2: Numerical and asymptotic results for (a) Ra_c and (b) k_c at $x = 3$. In (a) the dashed line is the asymptotic result (48).

The only solution is trivial unless the coefficient matrix in (50) is singular. This forms the basis of the method: searching for combinations of Ra_c and k so that the determinant of this coefficient matrix is zero.

For a fixed temperature profile $T_0(z, t)$ the aim is to find the lowest Ra_c and corresponding k_c that makes the determinant of the coefficient matrix in (50) zero. The numerical procedure uses the MATLAB function `fminbnd` to minimise over k a function that finds Ra_c so that the determinant of the coefficient matrix in (50) is zero for fixed k . This function first steps up from $Ra_c = 0$ until a zero is bracketed. The function then uses the MATLAB routine `fzero` to locate Ra_c for a particular k . A side product of the procedure is the eigenfunction associated with each Ra_c and k_c pair. This can be used to characterise the secondary motion as single or double celled convection.

Results and Discussion

Fig 2 shows typical results for the evolution of Ra_c and k_c at $x = 3$. Initially as heat is added the water column becomes increasingly unstable which is shown via the initially decreasing Ra_c in fig 2(a). This decrease continues until the surface temperature reaches 1 (at $t \approx 1.2$) after which adding heat leads to a stable and thickening surface layer. As the thickness of this layer increases Ra_c also increases. The transition from decreasing to increasing Ra_c occurs within the $k_c = 0$ regime which means the asymptotic results capture this transition.

Once the stable layer has grown sufficiently the $k \rightarrow 0$ results are no longer valid. For $x = 3$ this happens at $t \approx 2.7$ (see fig 2(b)). This time also corresponds to the numerical and asymptotic calculations of Ra_c diverging in fig 2(a). Physically, the stable surface layer has isolated the unstable deeper layer from the insulated boundary condition at $z = 0$.

Another transition occurs in the stability problem. Fig 3 shows two profiles of u_0 , the eigenfunction associated with the secondary motion. Note that at $t = 2$ the numerical and asymptotic profiles shown in fig 3 are indistinguishable. However the profile at $t = 3.5$ is in a region where the $k \rightarrow 0$ results are not valid and the asymptotic result is not shown. The profile for $t = 2$ (dashed line) shows that the secondary motion consists of a single cell that encompasses the entire depth. The profile at $t = 3.5$ (solid line) has a double cell structure with a smaller, weaker cell sitting at the surface. The transition from single to

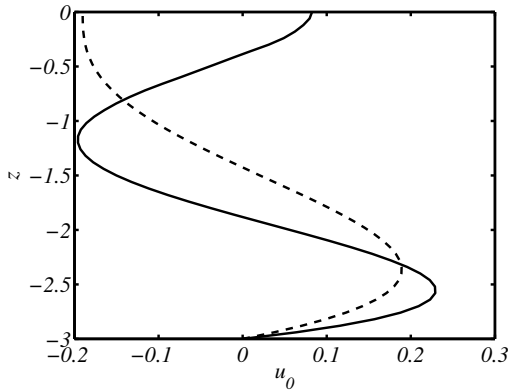


Figure 3: Two profiles of u_0 at $x = 3$ from the numerical calculations showing the transition from single cell ($t = 2$, dashed line) to double cell ($t = 3.5$, solid line).

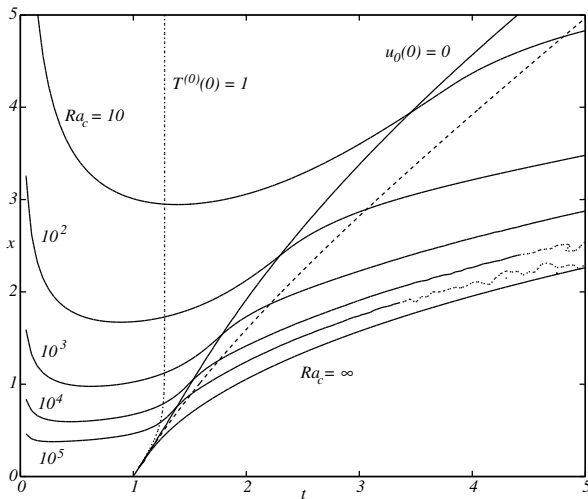


Figure 4: Contours of the numerically calculated Ra_c in the (t, x) -plane for $\eta = 1$ and $\sigma = 10$. The $Ra_c = \infty$ contour is determined by points where $T^{(0)}|_{z=-x} = 1$. Also shown is the location where the surface temperature $T^{(0)}|_{z=0}$ equals 1 (dotted line), the location where $u_0|_{z=0} = 0$ (solid line) and the location where the vertically averaged temperature is 1 (dashed line).

double cell circulation can be characterised by the surface velocity $u_0|_{z=0}$ being zero. This transition happens just before k_c becomes non-zero so it is captured by the asymptotic results.

Fig 4 summarises the results of this paper. It shows contours in the (t, x) -plane of the numerically calculated Ra_c . It also includes the $Ra_c = \infty$ contour which corresponds to the points where $T^{(0)}|_{z=-x} = 1$. For points in the (t, x) -plane below this contour the water column is stably stratified over the entire depth. For points above this contour secondary motion can be expected if Ra exceeds the critical value associated with that point. Note that the numerically calculated contours become inaccurate near the $Ra_c = \infty$ contour (indicated by the dotted contours in Fig 4).

For a fixed distance from the shore the passage of the thermal bar system is marked by a number of transitions. First the surface temperature reaches 1 which marks the establishment of a stable surface layer. Despite there being a stable surface layer

the water column is still unstable over its entire depth with the secondary motion consisting of a single cell encompassing the entire depth of the water column. The next transition is from single- to double-celled secondary motion. Here, the water column does not turn over its entire depth. This means that the stable surface layer is not mixed with the deeper parts of the water column and in a lake this marks the establishment of a permanent surface layer. This happens before the vertically averaged temperature has reached 1, the traditional marker of the arrival of the thermal bar. The final transition to summer conditions is when the temperature of the entire water column becomes greater than 1 after which the present model predicts no secondary motion.

Concluding Remarks

This paper has presented a framework for the evolution of the thermal bar system that is based on the instantaneous stability of the local water column. This framework leads to the thermal bar apparently moving out from the shore at a slightly greater speed than the vertically mixed model of [4] despite there being no horizontal heat transfer in the model. The establishment of summer conditions is marked by a number of transitions as the stability characteristics of the warming water column evolve.

References

- [1] Chapman, C. J. and Proctor, M. R. E., Non-linear Rayleigh-Bénard convection between poorly conducting boundaries, *J. Fluid Mech.*, **101**, 1980, 749–782.
- [2] Drazin, P. G. and Ried, W. H., *Hydrodynamic Stability*, Cambridge Texts in Applied Mathematics, Cambridge University Press, Cambridge, 2004, 2nd edition.
- [3] Elliott, G. H., A mathematical study of the thermal bar, in *Proc. 14th Conf. Great Lakes Res.*, Intl Assoc. Great Lakes Res, 1971, 545–554, 545–554.
- [4] Elliott, G. H. and Elliott, J. A., Laboratory studies on the thermal bar, in *Proc. 13th Conf. Great Lakes Res.*, Intl Assoc. Great Lakes Res, 1970, 413–418, 413–418.
- [5] Farrow, D. E., An asymptotic model for the hydrodynamics of the thermal bar, *J. Fluid Mech.*, **289**, 1995, 129–140.
- [6] Farrow, D. E., A model of the thermal bar in the rotating frame including vertically non-uniform heating, *Environ. Fluid Mech.*, **2**, 2002, 197–218.
- [7] Roberts, A. J., An analysis of near-marginal, mildly penetrative convection with heat flux prescribed on the boundaries., *J. Fluid Mech.*, **158**, 1985, 71–93.
- [8] Zilitinkevich, S. S., Kreiman, K. D. and Terzhivik, A. Y., The thermal bar, *J. Fluid Mech.*, **236**, 1992, 27–42.